UCRL-JC-126834
PREPRINT

# Simulations of Laser-Initiated Stress Waves

**D. J. Maitland, P. Celliers, P. Amendt,
L. Da Silva, R. A. London, D. Matthews,
M. Strauss, and S. R. Visuri**

**This paper was prepared for submittal to the
Society of Photo-Optical Instrumentation Engineers BiOS '97
San Jose, California
February 8-14, 1997**

**March 7, 1997**

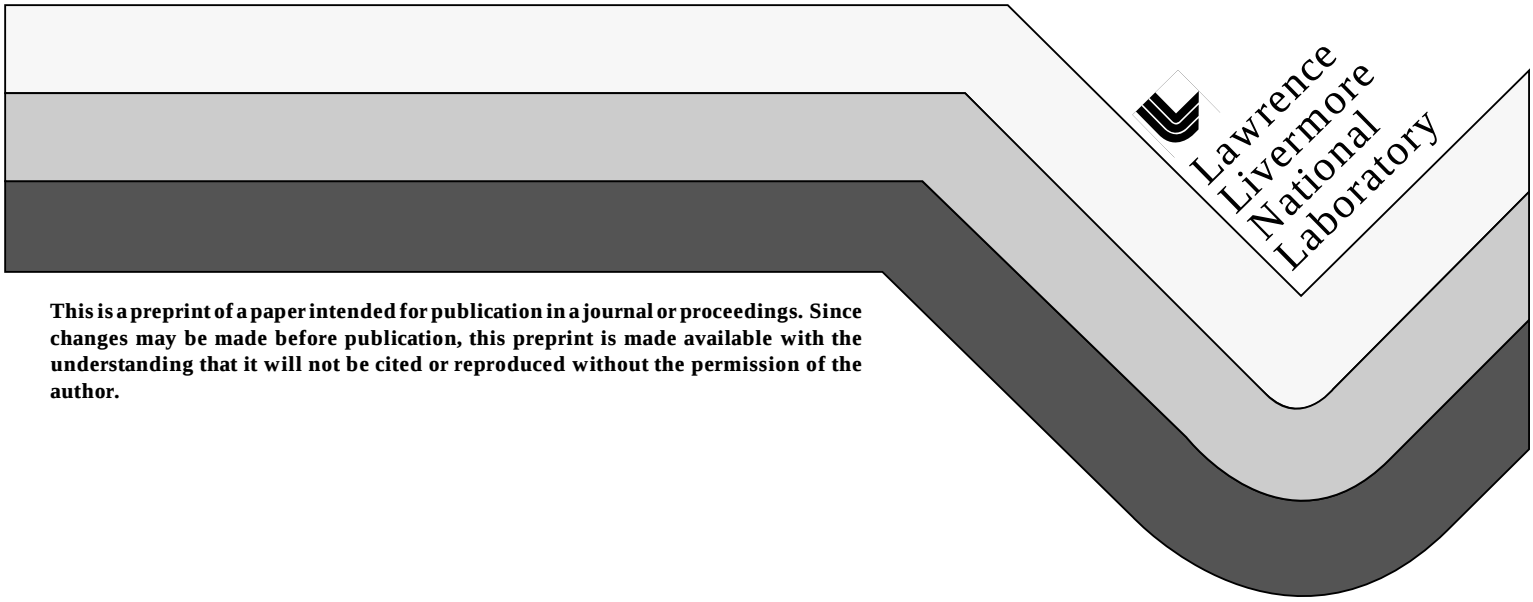

# Simulations of Laser-Initiated Stress Waves

Duncan J. Maitland, Peter Celliers, Peter Amendt, Luiz Da Silva,
Richard A. London, Dennis Matthews, Moshe Strauss‡ and Steven R. Visuri

Lawrence Livermore National Laboratory, Livermore, CA 94550;
‡Nuclear Research Center, Negev, P.O. Box 9001, Beer Sheva, Israel

## ABSTRACT

We present a study of the short-timescale (less than 250 ns) fluid dynamic response of water to a fiber-delivered laser pulse of variable energy and spatial profile. The laser pulse was deposited on a stress confinement timescale. The spatial profile was determined by the fiber core radius, r, (110 and 500 microns) and the water absorption coefficient, $\mu_a$, (200 and 50 1/cm). Considering 2D cylindrical symmetry, the combination of fiber radius and absorption coefficient parameters can be characterized as near planar ($1/\mu_a$ greater than r), symmetric ($1/\mu_a \approx r$), and side-directed ($1/\mu_a$ less than r). The spatial profile study shows how the stress wave varies as a function of geometry. For example, relatively small absorption coefficients can result is side-propagating shear and tensile fields.

## 2. INTRODUCTION

The evolution of stress waves emanating from laser energy deposited at the tip of an optical fiber is examined in this report. The influence of geometry on the stress wave features is demonstrated. For example, assuming that tension and shear are desirable stress wave features for a given clinical application, the selection of the fiber radius relative to the deposition depth can be chosen to optimize the tension and shear of the generated stress wave. The preliminary results provided by these simulations suggest that the compressive, tensile and shear characteristics of the stress wave can be engineered by controlling the absorption depth of the laser energy, the fiber tip geometry, and, implicitly, the deposited energy.

## 3. MODELING METHODS

The simulations were performed in two stages. The initial energy distribution at the fiber tip was calculated with a 2D axi-symmetric (r and z) Monte Carlo photon propagation code[1]. The Monte Carlo code was used to approximate the sharp radial cutoff of energy deposition while maintaining the appropriate exponential energy deposition along z. The calculated energy distribution was then used as an initial condition in the hydrodynamic computations performed by LATIS3D. Figure 1 shows a typical initial pressure distribution. The fiber was hydrodynamically modeled as a perfect reflector with zero normal-velocity fields. The region around the fiber was modeled as water with a Lawrence Livermore National Laboratory generated equation-of-state (EOS)[2]. After the fiber-water geometry was initialized, the hydrodynamic package was used to explicitly time-step the propagation of the stress wave that results from the energy deposition at the tip of the fiber. Figure 2 shows a snapshot at 150 ns after start of the problem depicted in Figure 1.

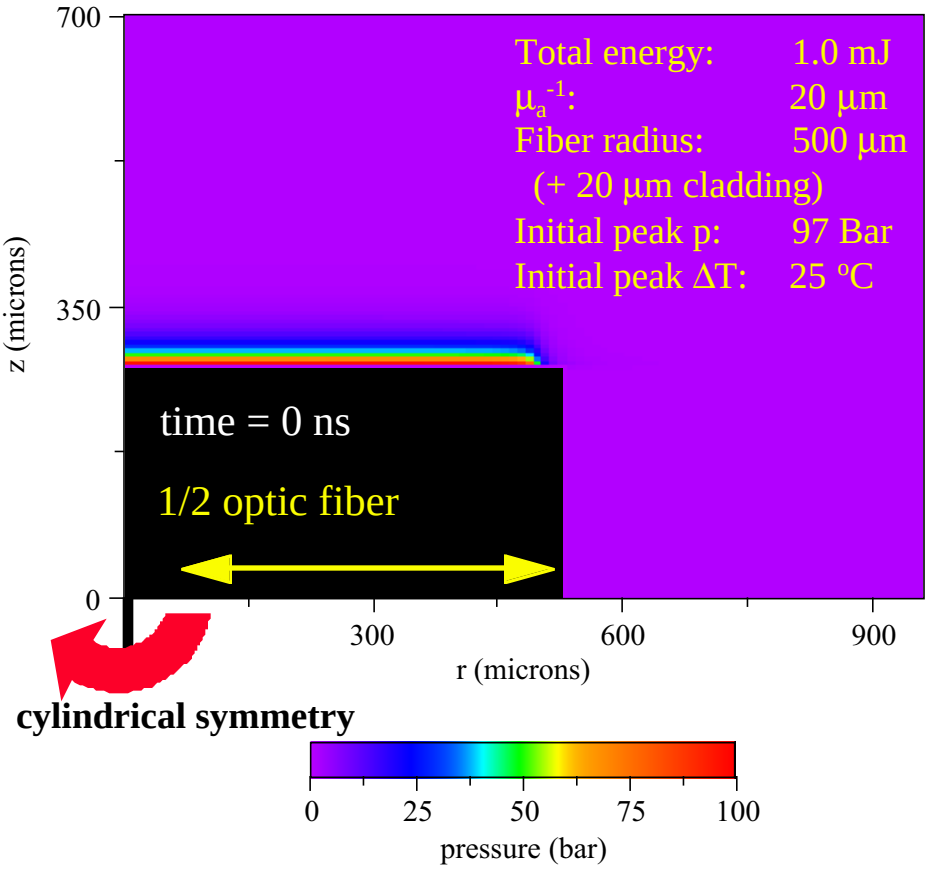


Figure 1. An example of the initial conditions used by the LATIS3D program. The cylindrical half-space is shown with the fiber depicted as the black region. The model uses a water equation-of-state in all other regions of the simulation.

LATIS3D is a discontinuous finite element code currently capable of implementing hydrodynamic, radiation diffusion and thermal diffusion physics. LATIS3D is a multi-physics simulation program that is similar to LATIS, which has previously been described[3]. The code names are based on an acronym standing for LAser-TISsue. The physics processes considered by the two codes are equivalent. However, LATIS3D is based on a developmental code, ICF3D[4,5]. The 2D hydrodynamic results presented here used arbitrary Lagrangian-Eulerian hydrodynamics with reflective boundary conditions. The hydrodynamic algorithm is based on the numerical solution to the mass, energy and momentum conservation equations along with the EOS table. The solution to the conservation equations results in time and space dependent values of pressure (p), density (ρ) and velocity (u). The EOS is used to look up the internal energy (e) and temperature (T) that correspond to p, ρ and u.

## 4. EXPERIMENTAL VALIDATION OF THE SIMULATIONS

As previously described, we used a Mach-Zehnder interferometer arrangement to provide a sensitive and quantitative measurement of the refractive index variations produced through the compression of the liquid within the stress transient[6]. The use of interferometry to measure the refractive index changes caused by stress field transients is a well known technique[7,8]. This analysis involves the generation of a two-dimensional phase distribution from the interferogram, followed by Abel inversion[9] to extract the three-dimensional refractive index distribution created by the stress wave. The final product of these experiments and analysis is a map of the refractive index changes (Δn) caused by the space and time dependent stress wave.

The experimentally generated Δn maps can be directly compared with similar maps generated from the simulation results. In water, the relationship between refractive index and density, temperature and wavelength is well known[10]. Hence, the simulations were converted into the refractive index maps.

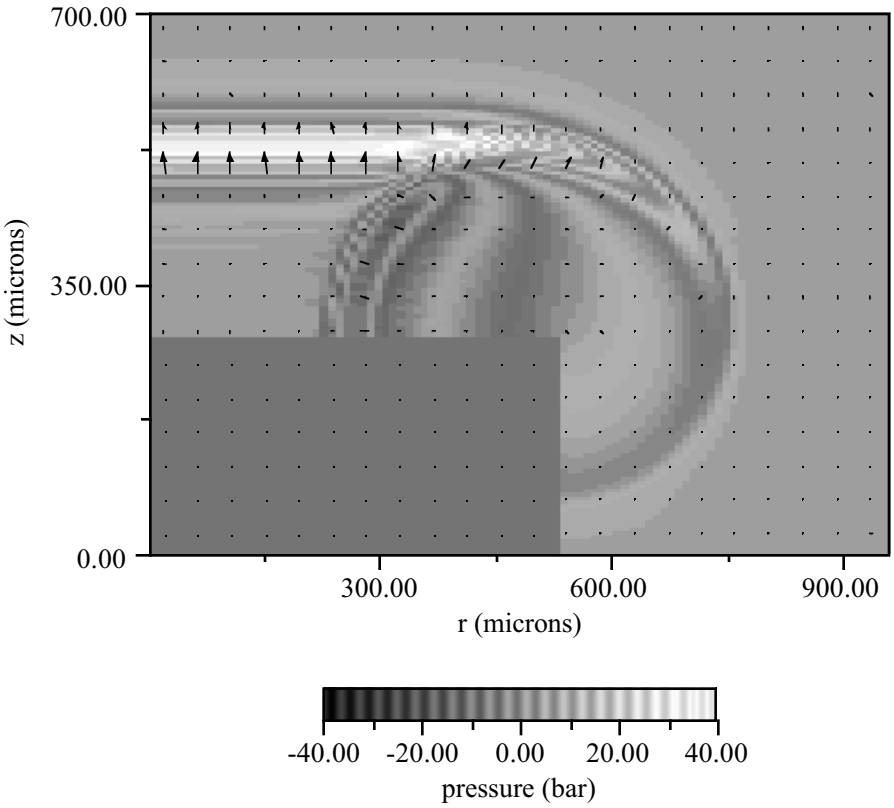


Figure 2. Stress wave at 150 ns. The pressure and relative velocity fields are shown for the problem described in Figure 1. Compression and tension are both observed. The velocity gradients perpendicular to the vector directions indicate shear fields. In soft tissue the shear fields shown would be qualitatively similar, but altered somewhat by the shear strength.

## 5. RESULTS

A qualitative comparison of experimental and simulated results is provided by the refractive index maps shown in Figure 3. The general characteristics agree well. The relaxation of the deposited, stress-confined energy produces a traveling compression wave that, due to the cylindrical symmetry, is followed by a tensile wave. Two noticeable differences between the experimental and simulated images are the geometry of the tensile wave and the deposition region. The experimental index map does not show that, at 250 ns after the laser was turned on, cavitation bubbles are formed within the deposition region. The water within the deposition region "failed" due to the tensile stresses acting on nucleation sites in the water. Our current belief is that the differences between the simulated and experimental tensile waves is due to the model's inability to account for the cavitation of the water. This will be remedied in the futyre since we have an ongoing effort to incorporate material strength and failure into LATIS and, eventually, LATIS3D[11]. The differences in the deposition region are, in part, also due to the cavitation bubbles' impact on refractive index (both density and temperature) in the deposition region. The simulations' sound speed is a few percent faster than the experiment. This error is a result of an incorrect compressibility in the EOS and will be corrected in future simulations.

The peak tensions in the measured and simulated index maps (Figure 3.) are approximately -150 bar each. Since no cavitation bubbles were noted outside the deposition region in the experiment, such tensile stresses did not cause "failure" in the water. Further, since the experimental and simulated tensile magnitudes are approximately equal (though the profiles are different), the simulation may be used to estimate that the tensile wave was -250 bar when it was just outside the deposition region. Thus an experimental wave of 30 ns in duration with a peak tension of -250 bar did not cause cavitation bubbles. Paltauf et.al. estimated that tensile waves of -10 bar or more would cause cavitation in water[12] , based on experiments with, approximately, a 300 ns-long tensile wave. In order to explain this difference, we postulate that the strength of water is a dynamic function of the pressure history.

Figure 4 presents the simulation results for two different geometric cases. The differences in the two cases (Figures 4a-4c or 4d-4f) exhibit the geometric influence on tensile and shear stresses. The geometry of the delivery system may be engineered to optimize stresses radially, for example, as in Figures 4d-4f. Figures 4a-4c are for the same case used in the Figure 3. index maps.

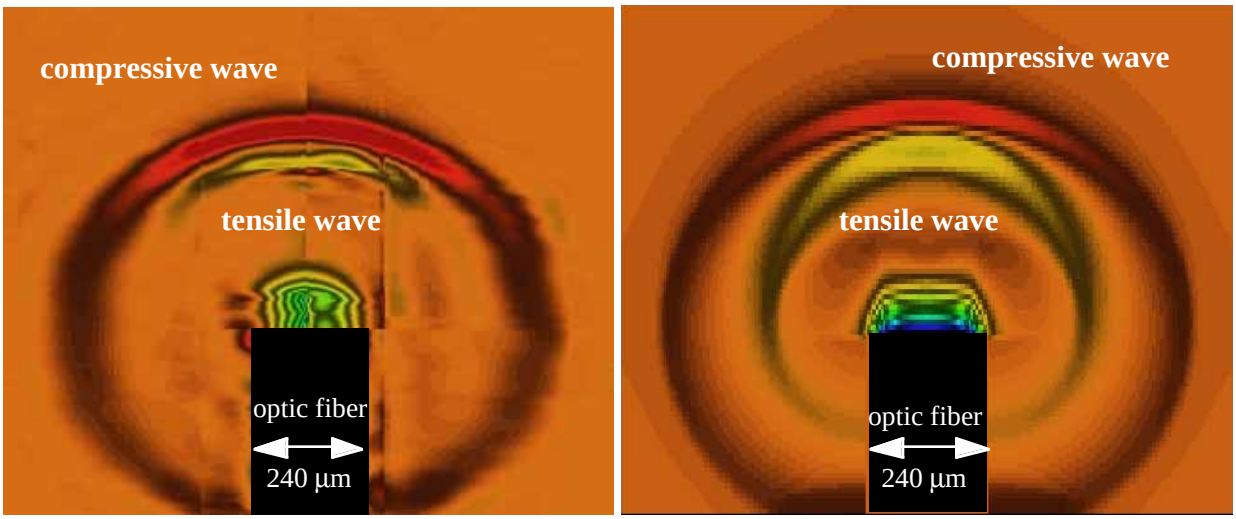


Figure 3. A comparison of experimental and simulated refractive index maps. The images are at 250 ns after the laser was turned on. The experimental pulse length was 5 ns. The energy deposited was 1.0 mJ into a 200 $cm^{-1}$ absorption coefficient. Both results exhibit similar qualitative characteristics for the leading compression wave, trailing tensile wave and energy deposition region. In both figures, the leading compression wave corresponds to approximately +200 bar and the trailing tensile wave approximately -150 bar.

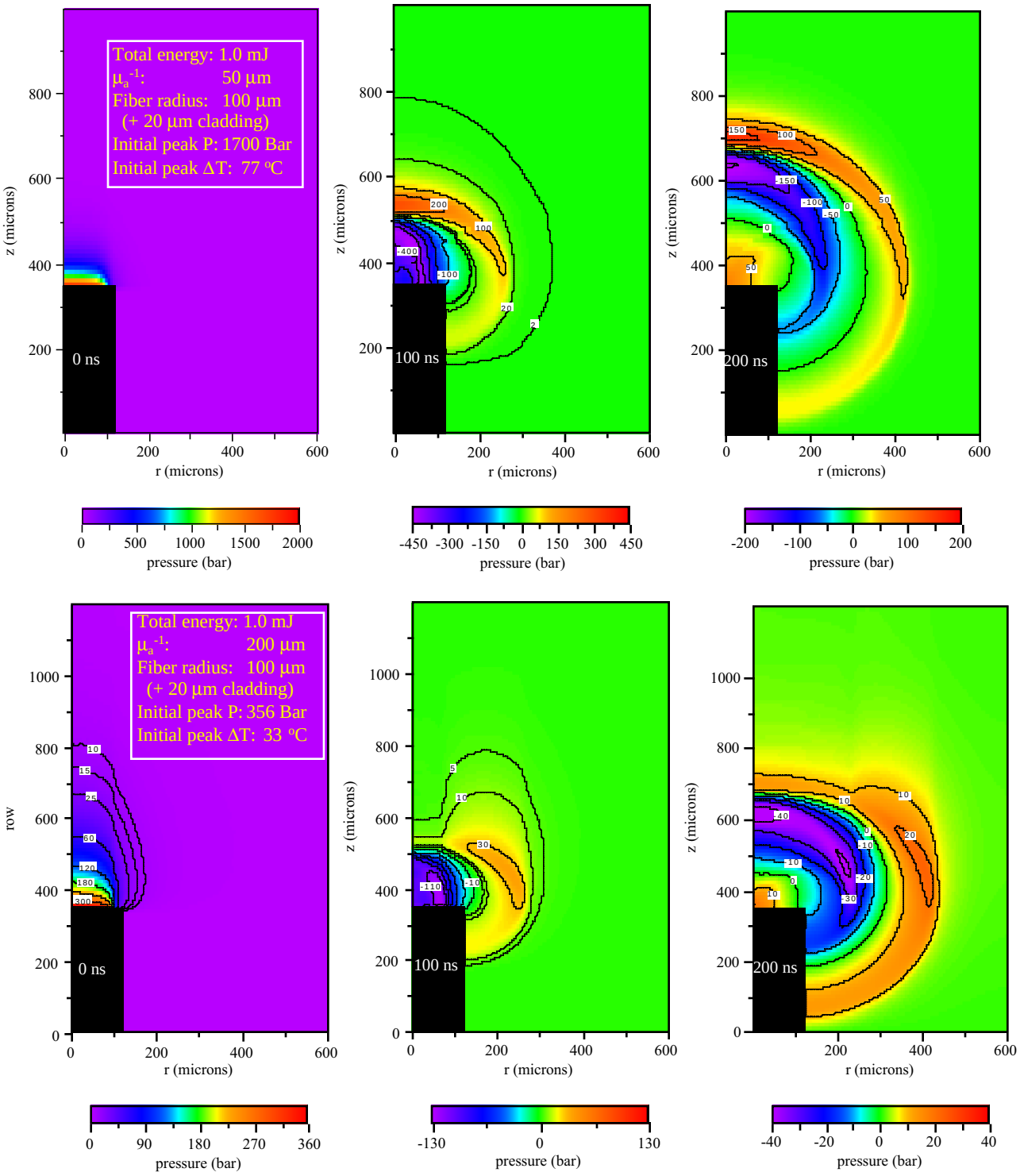


Figure 4. Simulated stress wave propagation from fiber tip. The smaller absorption coefficient, $\mu_a$, for figures d.-f. causes the peak stresses to be side-directed. Ignoring all other design factors, the location of the peak stress can be adjusted by the appropriate selection of $\mu_a$ and r, the fiber radius.

## 6. CONCLUSION

We have shown that LATIS3D can quantitatively predict the stress wave features for a laser-initiated stress wave propagating from an optic fiber. The refractive index maps also agree well with the experimental results. The results show how the energy delivery geometry, which is defined by the absorption coefficient and the fiber radius, influences the evolution of the stress wave.

## 7. ACKNOWLEDGMENTS

This work was performed under the auspices of the US. Department of Energy by the Lawrence Livermore National Laboratory under Contract W-7405-ENG-48.

## 8. REFERENCES

1. S.L. Jacques and L. Wang, "Monte Carlo Modeling of Light Transport in Tissues," in *Optical-Thermal Response of Laser-Irradiated Tissue*, (eds. A.J. Welch and M.J.C. van Gemert) pp. 73-100, Plenum Press, (1995).
2. D. A. Young and E. M. Corey, *J. Appl. Phys.* **78**, 3748, (1995).
3. R. A. London, M. E. Glinsky, G. B. Zimmerman, D. S. Bailey, D. C. Eder and S.L. Jacques, "Laser–Tissue Interaction Modeling with LATIS," submitted to Applied Optics, February, 1997.
4. A.I. Shestakov, M.K. Prasad, J.L. Milovich, N.A. Gentile, J.F. Painter, G. Furnish and P.F. Dubois, "The ICF3D Code," *Inertial Confinement Fusion Quarterly Report*, UCRL-LR-124418, in print (1997).
5. D.S. Kershaw, M.K. Prasad, M.J. Shaw, and J.L. Milovich, "3D unstructured mesh ALE hydrodynamics with the upwind discontinuous finite element method," submitted to *J. Comp. Phys.*
6. P. Celliers, L.B. Da Silva, N.J. Heredia, B.M. Mammini, R.A. London and M. Strauss, "Dynamics of laser-induced transients produced by nanosecond duration pulses," in *Lasers in Surgery: Advanced Characterization, Therapeutics and Systems VI* Proc. SPIE Vol. **2671**, pp. 22-27, Society of Photo-Optical Instrumentation Engineers (1996).
7. B. Ward and D.C. Emmony, "Interferometric studies of the pressures developed in a liquid during infrared-laser-induced cavitation-bubble oscillation," *Infrared Phys.*, **32**, pp. 489-515 (1991).
8. M. Kujawinska, "Spatial phase measurement methods," in Interferogram Analysis, (eds. D.W. Robinson and G.T. Reid) pp. 140-193, IOP Publishing Ltd., Bristol (1993).
9. W.R. Wing and R.V. Neidigh, "A rapid Abel inversion," Am. J. Phys., **39** pp.760-764 (1971).
10. I. Thormahlen, J.Straub , and U. Grigull, "Refractive index of water and its dependence on wavelength, temperature and density," *J. Phys. Chem. Ref. Data* **14**, 933-945 (1985)
11. M. Glinsky, R.A. London, and D. Bailey, "LATIS modeling laser-induced midplane and backplane spallation," in *Laser-Tissue Interactions VIII* Proc. SPIE Vol. **2675**, Society of Photo-Optical Instrumentation Engineers (1997).
12. G. Paltauf, E. Reichel and H. Schmidt-Kloiber, "Study of different ablation models by use of high-speed-sampling photography," in *Laser-Tissue Interactions III* Proc. SPIE Vol. **2675**, pp. 343-352, Society of Photo-Optical Instrumentation Engineers (1992).

*Technical Information Department* • **Lawrence Livermore National Laboratory**
**University of California • Livermore, California 94551**